

Network and Experimental Pharmacology to Decode the Action of Wendan Decoction Against Generalized Anxiety Disorder

Qi Jin^{1,*}, Jie Li^{2,*}, Guang-Yao Chen^{1,*}, Zi-Yu Wu³, Xiao-Yu Liu², Yi Liu⁴, Lin Chen⁵, Xin-Yi Wu⁵, Yan Liu², Xin Zhao², Yue-Han Song²

¹Graduate School, Beijing University of Chinese Medicine, Beijing, 100029, People's Republic of China; ²School of Traditional Chinese Medicine, Beijing University of Chinese Medicine, Beijing, 100029, People's Republic of China; ³Dongzhimen Hospital, Beijing University of Chinese Medicine, Beijing, 100007, People's Republic of China; ⁴Humanities School, Beijing University of Chinese Medicine, Beijing, 100029, People's Republic of China; ⁵Qihuang School, Beijing University of Chinese Medicine, Beijing, 100029, People's Republic of China

*These authors contributed equally to this work

Correspondence: Xin Zhao; Yue-Han Song, Email zhaoyyx@sohu.com; songyuehan1981@126.com

Objective: The mechanism of Wendan Decoction (WDD) against Generalized Anxiety Disorder (GAD) was predicted by network pharmacology and validated by in vivo and in vitro experiments.

Methods: The targets of WDD for the treatment of GAD were obtained by a search of online databases. Further, PPI network and KEGG enrichment were used to identify the key targets and pathways. Ultimately, these key targets and pathways were validated by in vivo experiments on GAD mice modeled by repeated restraint stress (RRS) and in vitro experiments on inflammatory factor stimulated BV-2 cells.

Results: Through searching the databases, the 137 ingredients of WDD that correspond to 938 targets and 4794 targets related to GAD were identified. Among them, 569 overlapping targets were considered as the therapeutic targets of WDD for GAD. PPI analysis showed that the inflammation-related proteins IL-6, TNF, SRC and AKT1 were the key targets, and KEGG enrichment suggested that PI3K/AKT and MAPK signaling pathways were key pathways of WDD in the treatment of GAD. In vivo experiments, RRS mice exhibited abnormality in behavioristics in open field test (OFT) and elevated plus maze (EPM) and increases in serum corticosterone and the percentage of lymphocytes positive for IL-6 in peripheral blood. These abnormal changes can be reversed by WDD and the positive control drug paroxetine. In vitro experiments, WDD can inhibit IL-6 induced activation of PI3K/AKT and MAPK signaling pathways in BV2 cells, and suppress the ensuing release of inflammatory factors TNF- α , IL-1 β and PGE₂, and showed a dose-dependent effect.

Conclusion: WDD is able to resist GAD by relieving inflammatory response in peripheral and central system.

Keywords: Wendan Decoction, Generalized Anxiety Disorder, network pharmacology, Interleukin-6, PI3K/AKT signaling pathway, MAPK signaling pathway

Introduction

Generalized Anxiety Disorder (GAD) is one of the most common anxiety disorders characterized by continuously significant nervousness, autonomic hyperfunction and neuromuscular motor disturbance.¹ According to a globally joint cross-sectional epidemiological survey, 3.7% of people have suffered from GAD during their lives, and most of GAD patients had concurrent mood disorders such as major depression.^{2,3} According to epidemiology and health economics research, GAD has become a major socio-economic burden for health-care systems during the past 30 years.⁴

Selective Serotonin Reuptake Inhibitor (SSRIs) and Serotonin-norepinephrine reuptake Inhibitor (SNRIs), such as paroxetine and venlafaxine, are first-line therapeutic agents for GAD.⁵ However, most drugs have serious side effects, including nausea, constipation, insomnia and liver damage.⁶ Nowadays, the research and development of anxiolytic

medication and alternative therapy has become a hot research topic.^{7,8} Traditional Chinese medicine (TCM) has been used to treat mental and nervous system disorders for thousands of years, with the characteristics of multi-target and multi-channel due to their complex compositions. Several randomized controlled trials (RCT) have shown that TCM prescriptions such as Xiao Yao San, Renshu Powder and Qingyan Formula, have prominent therapeutic effects against GAD.^{9–11}

Wendan Decoction (WDD) is a representative formula for treating mental and neurological disorders, such as schizophrenia, insomnia and melancholia.^{12–15} It consists of Banxia (*Pinellia ternata* (Thunb.) Makino) (6 g), Zhishi (*Citrus aurantium* L.) (6g), Chenpi (*Citrus reticulata* Blanco) (9g), Zhuru (*Bambusa tuldoidea* Munro) (6g), Fuling (*Poria cocos* (Schw.) Wolf) (4.5g), Shengjiang (*Zingiber officinale* Roscoe) (6g), Dazao (*Ziziphus jujuba* Mill.) (3g) and Gancao (*Glycyrrhiza uralensis* Fisch. ex DC.) (3g), first composed by Wuze Chen, a TCM physician in 12th century. Several RCTs show that WDD can effectively improve the symptoms of anxiety patients, reduce the scores of Hamilton Anxiety Scale (HAMA) and Self-Rating Anxiety Scale (SAS), with good safety and efficacy.^{16,17} However, the holistic mechanism of WDD against GAD has not been fully revealed.

Network pharmacology, integrating systems biology and pharmacology, provides a new approach to understand the relationship between Chinese herbal prescription and disease at a systematic level.¹⁸ It is a reliable and rapid method not only contributing to exploration of active ingredients in the prescription, but also providing prediction of potential targets and pathway. In this study, network pharmacology was applied to explore the mechanisms of WDD for the treatment of GAD. In vivo and vitro experiments were used to confirm the reliability of network pharmacology.

Materials and Methods

Network Pharmacology Prediction

Collection of Active Ingredients and Targets

Ingredients of WDD and corresponding targets were extracted from Traditional Chinese Medicine Systems Pharmacology database (TCMSP, <http://tcmsp.com/tcmsp.php/>)¹⁹ and The Encyclopedia of Traditional Chinese Medicine database (ETCM, <http://www.nrc.ac.cn:9090/ETCM/>).²⁰ Pubchem database (<https://pubchem.ncbi.nlm.nih.gov/>)²¹ and SwissTargetPrediction database (<http://www.swisstargetprediction.ch/>)²² were also used for the identification of putative targets. Unified Protein Database database (UniProt, <https://www.uniprot.org/>)²³ was used for target standardization and annotation. The gene targets of disease were extracted from GeneCards database (<http://www.genecards.org/>)²⁴ and Online Mendelian Inheritance in Man database (OMIM, <https://omim.org/>)²⁵ with “Generalized Anxiety Disorder” as the keyword. We received an ethics committee waiver for using these two databases from Medical and Animal Experiment Ethics Committee of Beijing University of Chinese Medicine. A herb-target network was constructed using Cytoscape 3.7.2 software²⁶ to present the distinction of both the known targets and the putative targets.

Network Construction and Analysis of Protein-Protein Interaction (PPI)

In order to identify the key targets in WDD-GAD intersection genes, STRING database (<https://string-db.org/>)²⁷ and Cytoscape 3.7.2 software were used to construct and analyze the PPI network. In STRING database, organism was set as *Homo Sapiens*, and confidence was set as greater than 0.9, while disconnected nodes were hidden in the network. Consequently, subnetwork was constructed as their degree values became twofold the median degree of all nodes in the network.²⁸ A network topology analysis (NCA) on the related targets of WDD was carried out. Four topological features, Betweenness Centrality (BC), Closeness Centrality (CC), Degree Centrality (DC) and Eigenvector Centrality (EC) were calculated to filter out the key targets in the subnetwork by cytoNCA app.²⁹

Kyoto Encyclopedia of Genes and Genomes (KEGG) Enrichment Analysis

KEGG enrichment analysis was performed on the therapeutic targets of WDD for GAD by STRING database, which is critical to exploring pathogenesis and therapy of WDD treating GAD. In order to illustrate the complex pharmacological network of WDD more accurately, the “disease” and “metabolism” category of the KEGG terms were removed according to KEGG database (<https://www.kegg.jp/>),³⁰ and top 15 KEGG pathways of WDD are displayed in a bubble chart according to the ascending order of P value.

Experimental Verification

Reagents and Antibodies

The reagents and antibodies used in this study are as follows: RPMI 1640 medium (Gibco, USA), Fetal bovine serum (FBS, ScienCell, USA), Leukocyte activation cocktail with Golgi Plug (552843, BD, USA), 0.25% trypsin-EDTA (Gibco, USA), penicillin streptomycin (Gibco, USA), Recombinant Murine IL-6 (216-16, peprotech, USA), Dexamethasone (DEX) (sigma, USA), DMEM medium (Gibco, USA), phosphate-buffered saline (PBS, HyClone, USA), RIPA lysis buffer (Solarbio Life Sciences, China), Phenylmethane sulfonyl fluoride (PMSF) (Solarbio Life Sciences, China), Phosphatase inhibitor (Beyotime, China), CellTiter 96[®] AQueous One Solution Cell Proliferation Assay (G358A, Promga, USA), Corticosterone ELISA Kit (EIA-4164, DRG, Germany), Prostaglandin E₂ ELISA Kit (EIA-5811, DRG, Germany), TNF- α (CME0004, Beijing 4A Biotech), IL-1 β (CME0015, Beijing 4A Biotech), Formic acid (A117-50, Fisher Chemical, USA), Acetonitrile (A955-1, Fisher Chemical, USA).

PerCP/Cyanine5.5 anti-mouse CD3 Antibody (100218, BioLegend, USA), FITC anti-mouse CD4 Antibody (116004, BioLegend, USA), PE anti-mouse IL-6 Antibody (504504, BioLegend, USA), PI3K antibody (A4992, Abclonal, China), Phospho-PI3K (Y467/199) antibody (YP0224, Immunoway, USA), AKT antibody (ab8805, Abcam, UK), Phospho-AKT (S473) antibody (4060S, Cell Signaling, USA), p38 MAPK (AP0526, Abclonal, China), Phospho-p38 MAPK (A14401, Abclonal, China), β -Actin antibody (AC026, Abclonal, China), HRP conjugated goat anti-rabbit IgG (ZB-2301, Zhongshan Jingqiao Biotechnology, China).

Preparation of Drugs

WDD was purchased from China Beijing Tongrentang Co., Ltd, consisting of the following eight herbs: Banxia (Pinellia ternata (Thunb.) Makino) (6 g), Zhishi (Citrus aurantium L.) (6g), Chenpi (Citrus reticulata Blanco) (9g), Zhuru (Bambusa tuldoidea Munro) (6g), Fuling (Poria cocos (Schw.) Wolf) (4.5g), Shengjiang (Zingiber officinale Roscoe) (6g), Dazao (Ziziphus jujuba Mill.) (3g) and Gancao (Glycyrrhiza uralensis Fisch. ex DC.) (3g). The freeze-dried powder of WDD was prepared as follows: The raw herbs were soaked in nine times their weight in water for 30 min, then decocted for 1h and filtered; the process was repeated twice. The filtrates from the three procedures were mixed and concentrated to 60 mL. Anhydrous ethanol enables macromolecules such as starch to deposit via alcohol precipitation.³¹ When the concentrated solution of WDD cooled down to room temperature, an equal volume of anhydrous ethanol (60mL) was added slowly and mixed thoroughly, kept refrigerated for 12 hours at 4°C. After centrifuging, the supernatant was obtained and then heated to 60±5°C to volatilize ethyl alcohol until the mixture became a density of 1.08g·cm⁻³.³² After that, WDD was freeze-dried into powder by a lyophiliser (SCIENTZ-10N, Ningbo scientz biotechnology Co., Ltd., China) and stored in a refrigerator at -20°C. The positive control drug Paroxetine for animal experiments was purchased Zhejiang Huahai Pharmaceutical Co., Ltd.

Drug Identification and Dissolution

The freeze-dried powder of WDD was detected by liquid chromatography tandem mass spectrometry (LC-MS) to ensure that freeze-dried powder contains all key ingredients as predicted by network pharmacology. After being sterilized with 0.22 μ m micro membrane filtration, WDD extract was used for ingredient identification on Nexera High-Performance Liquid Chromatograph (Japan Shimadzu Co., Ltd) coupled to the SCIEX 5600 Triple-TOF mass spectrometer (Sciex, Toronto, Canada). The LC-MS raw data was processed in MS-DIAL 4.60 software.³³ Ingredients were identified from the perspective of sample information, peak name, retention time, mass-to-charge ratio (m/z) and peak area, by searching several mass spectral reference libraries, including MassBank (<https://massbank.eu/MassBank/>),³⁴ RIKEN MSn spectral database for phytochemicals (ReSpect, <http://spectra.psc.riken.jp/>)³⁵ and Global Natural Products Social Molecular Networking (GNPS, <https://gnps.ucsd.edu/ProteoSAFe/static/gnps-splash.jsp>).³⁶

Assuming the average human weighs 60 kg, the therapeutic dose of WDD for an adult is 0.725g/kg/d (raw herbs). According to the ratio of mice to human body surface area, mice dose is 9.1-fold higher than human therapeutic doses, thus the mice dose is 6.5975g/kg/d (raw herbs).³⁷ Correspondingly, the dose of paroxetine for a mouse is 0.0303mg/g/d. WDD and paroxetine were dissolved in distilled water and kept in 4°C until use.

Animals Feeding and Administration

A total of 40 male BALB/c mice (20±2 g) were purchased from Beijing Vital River Experimental Animal Science and Technology Co., Ltd (License No. SCXK (Jing) 2021–0006; Beijing, China). The mice were housed in a Specific Pathogen Free (SPF) facility at China-Japan Friendship Hospital, where the condition was in accordance with the National Standards for Laboratory Animals of China (GB 14925–2010). Since the animal experiment was carried out in China-Japan Friendship Hospital, the experiment was approved by the experimental animal care and welfare ethics committee of China-Japan Friendship Hospital (No.zryhyy-21-21-07-12).

After one-week adaptive feeding, 40 mice were randomly divided into blank control group, repeated restraint stress (RRS) model group, WDD group and paroxetine group. RRS was conducted by placing mice in a 50-mL conic plastic tube for 4 hours from 9:00 a.m. to 13:00 p.m. every day. Blank control group mice received no restraint stress, while mice in model group, WDD group and paroxetine group received a 14-day course of RRS.³⁸ Drug administration was conducted by gavage an hour after the end of restraint stress. beginning from 8th day to 14th day of RRS, the mice in the blank control group and RRS group received a gavage of equivalent volume distilled water every day. And the daily gavage of WDD extract or paroxetine for a mouse in the WDD or paroxetine group.

After 14-day administration, behavioral tests were carried out.³⁹ Then, the mice were anesthetized with isoflurane, and blood samples were obtained from abdominal aorta in heparin tube. Of whole blood samples, 200ul were used for flow cytometry assays. The remaining blood samples were centrifuged to isolate the plasma, which was used for detection of corticosterone concentration by Enzyme-linked immunosorbent assay (ELISA). After collection of blood samples, the mouse was sacrificed for CO₂ asphyxiation.

Cell Culture and Drugs Administration

Bv2 cells (CS0271) were purchased from *Beijing Dingguo Changsheng Biotechnology Co.Ltd.* China. After resuscitation, Bv2 cells were cultured in DMEM complete medium (containing 90% DMEM, 10% FBS, 100 U/mL penicillin and 100 µg/mL streptomycin) in a standard cell culture incubator (5% CO₂, 37°C).⁴⁰ Once monolayer cell confluence was observed, the cell passage was carried out at a ratio of 1:2–1:3 with 0.25% EDTA-trypsin digestion.

In vitro, WDD powder was dissolved in PBS to different concentrations and added to cell culture medium. In order to determine the maximum tolerated dose, the MTS assay was employed to test cell viability.⁴¹ Subsequently, 1×10⁶ cells were seeded into 6-well plates and allowed to attach overnight. After being completely adherent, the cells were then pretreated with WDD and the positive control drug DEX for 1 h. 10 ng/mL of IL-6 was then added to induce a pro-inflammatory phenotype. Following 12-hour incubation, the culture supernatant was analyzed using ELISA assay and the cells were lysed for western blot (WB) assay.

Behavioral Tests

Open field test (OFT) and elevated plus maze (EPM) were employed to examine anxiety-like behaviors of mice. All the mice were placed in the behavior laboratory for 1 hour to habituate themselves to the environment before tests.⁴²

Open-field apparatus with a camera right above consisted of a 50 cm³ cube space, whose floor was evenly divided into 25 zones (9 central zones and 16 surrounding zones).⁴³ At the beginning of the experiment, the mice were deposited in the center of the open-field apparatus with the camera turning on to record the 5-minute track of each mouse. All the videos were analyzed using a professional software system (Ethovision XT 15, Noldus).

EPM apparatus consisted of two oppositely positioned open arms (66cm×5cm), two oppositely positioned enclosed arms (66cm×5cm) and a central square platform (5cm×5cm) from which four black arms radiated.⁴⁴ The maze was elevated to a height of 50 cm from the floor. Mice were placed individually into the central platform facing toward an open arm and allowed free exploration of the apparatus. An arm entry was defined as the entry of two fore limbs into one arm.

ELISA

The plasma corticosterone and cell supernatant were analyzed for TNF-α, IL-1β and PGE₂ by commercialized ELISA kit according to the instruction.^{45,46} The optical density (OD) value of each sample was read at 450 nanometers by a microplate reader. A standard curve was plotted according to OD of the concentration of standards by CurveExpert 1.4. The concentration of each sample were calculated with reference to a standard curve.

Flow Cytometry

Percentage of IL-6⁺CD3⁺CD4⁺ lymphocytes cells was examined by flow cytometry. 200µL blood sample was mixed with 200µL RPMI-1640 complete medium. Lymphocytes were stimulated by leukocyte activation cocktail and Golgi plug and incubated for 6 hours.⁴⁷ Subsequently, CD3 and CD4 antibodies were added into the sample for 15-minutes incubation. After lysing erythrocytes and fixing monocytes, the sample was added IL-6 antibody and incubated again in the dark at 4°C for 30 minutes. Finally, the samples were analyzed using the LSRFortessa flow cytometer (BD LSRFortessa, Becton, Dickinson and Company, USA).

Cell Viability Assay

Cell viability was measured by MTS assay. Bv2 cells were diluted to a concentration of 5×10^4 cells/mL. The cell suspensions were seeded in a 96-well plate, with 100 µL in each well at an average density of 5×10^3 cells per well. After the cells adhered to the wall, WDD was added to each well to final concentrations of 100, 200, 300, 400, 500, 600, 700, 800, 900 and 1000 µg/mL. After incubation 12 hours, the medium was replaced by fresh complete DMEM complete medium 100 µL per well. Another 2-hours incubation later, each well was added 20 µL MTS. Incubation was continued for an additional 2 hour, and the optical density (OD) value was measured with a microplate reader at 490 nm wavelength. Cell viability was calculated according to the equation following: viability (%) = $100 \times (\text{OD of treated sample} - \text{OD of medium}) / (\text{OD of control sample} - \text{OD of medium})$. The high dose was defined as the maximum concentration of WDD extract that had no effect on cell proliferation compared with blank group. Half maximal concentration was defined as a medium dose, and one quarter of maximal concentration was defined as a low dose.⁴¹

Western Blot

After the intervention, cells were washed with PBS and lysed with RIPA lysis buffer (containing 1%PMSF and 1% phosphatase inhibitor) on ice for 30 minutes. The supernatant was collected after centrifugation. Protein concentration was performed via the bicinchoninic acid (BCA) method.⁴⁸ The concentration of each extracted sample was corrected. Quantified proteins were mixed with 5×loading buffer and boiled at 100°C for 10 minutes. The samples were sub-packed and stored at -80°C until use.

Proteins were separated by SDS-PAGE gel electrophoresis under 120V and transferred to PVDF membranes on ice-bath under 80V, 50min. Afterwards, PVDF membranes were blocked with 5% skimmed milk powder in TBST at room temperature for 1 h. The membranes were incubated with primary antibody at 4°C overnight and secondary antibody for 1 hour at room temperature. Finally, blot visualization was carried out by chemiluminescence imaging system (ChemiScope 6100, Shanghai Qinxiang Scientific Instrument Co., Ltd). The grey value was measured by Image J software.⁴⁹

Statistical Analysis

Experimental data were analyzed by unpaired two-tailed Student's t-tests of the means between two groups. GraphPad Prism software version 5.01 (GraphPad Software Inc., CA, United States) was utilized to determine the statistical significance in comparisons. A P value of <0.05 was set for statistical significance. All the error bars shown in figures represent standard error of the mean (SEM).

Results

Ingredients and Targets of WDD

A total of 137 ingredients were screened out from TCMSP and ETCM, and detailed chemical parameters of all ingredients in each herb are listed in [Supplementary Table 1](#). The 137 ingredients of 8 herbs corresponding to 938 targets ([Supplementary Table 2](#)), 4794 targets related to GAD were identified ([Supplementary Table 3](#)). Among them, 569 targets overlap ([Supplementary Table 4](#)), which were considered the therapeutic targets of WDD against GAD. Medicine composition of WDD, the therapeutic targets of WDD against GAD and their relationship are presented in [Figure 1](#).

Construction and Analysis of Protein-Protein Interaction (PPI)

The therapeutic targets of WDD against GAD were input into STRING database and subjected to PPI analysis. PPI network was constructed based on confidence >0.9 and Degree Centrality topology analysis was performed on the

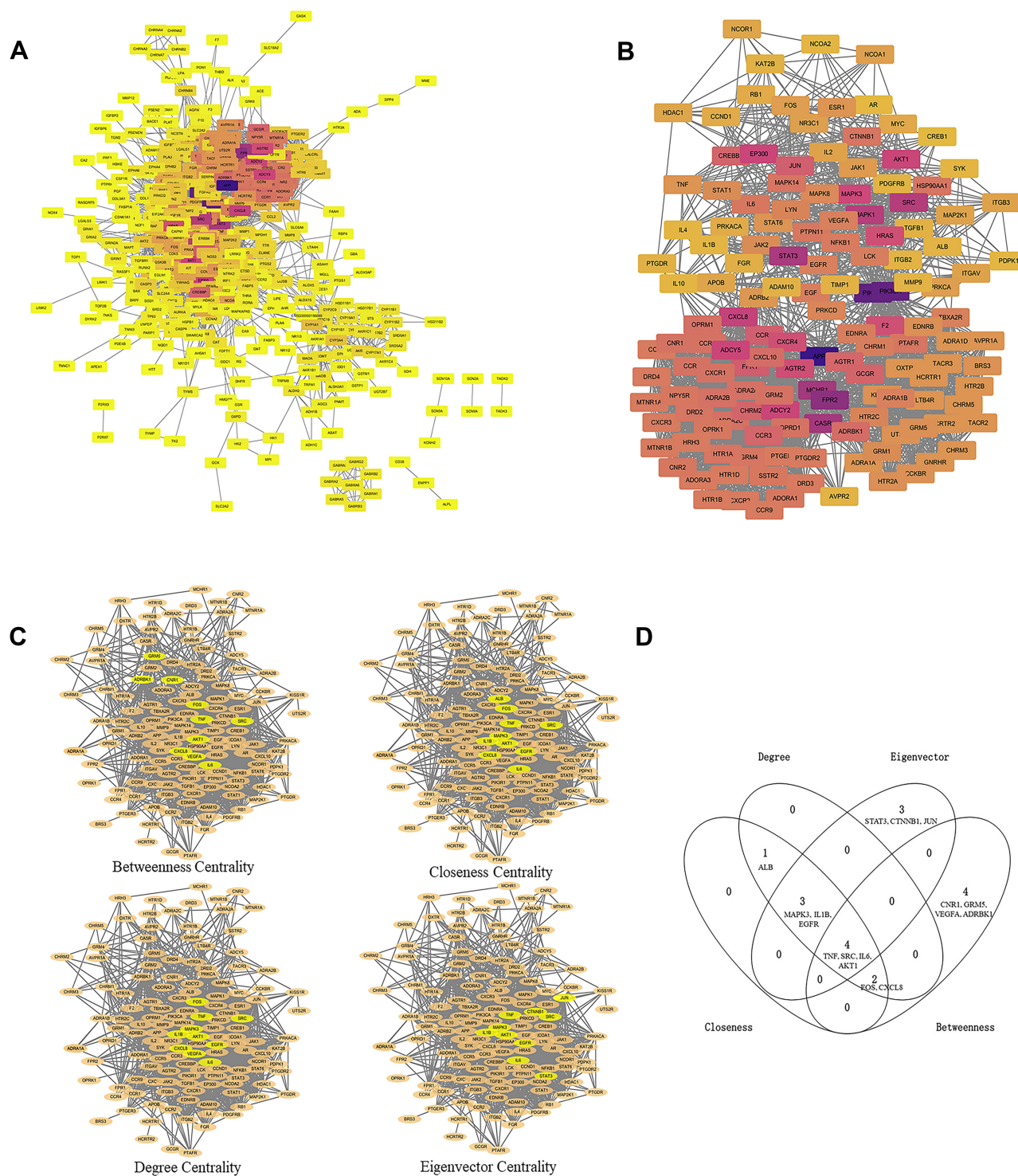


Figure 2 PPI topological analysis of Wendan Decoction treating Generalized Anxiety Disorder. **(A)** PPI network of 569 targets. **(B)** The subnet of PPI with 142 hub targets screened based on twice medium degree. **(C)** According to the Betweenness Centrality, Closeness Centrality, Degree Centrality and Eigenvector Centrality separately, TOP 10 targets in subnet from each criterion were labeled yellow. **(D)** Venn diagram of 4 topological analysis data. TNF, SRC, IL-6 and AKT1 were common targets.

Bambusa tuldoides Munro; hederagenin of *Poria cocos* (Schw.) Wolf; beta-sitosterol of *Zingiber officinale* Roscoe; quercetin and beta-sitosterol of *Ziziphus jujuba* Mill.; glabridin, quercetin and naringenin of *Glycyrrhiza uralensis* Fisch. ex DC. LC-MS detection suggested that they were all available in the samples of WDD we prepared (Figure 4), with specific information for each ingredient shown in Table 1.

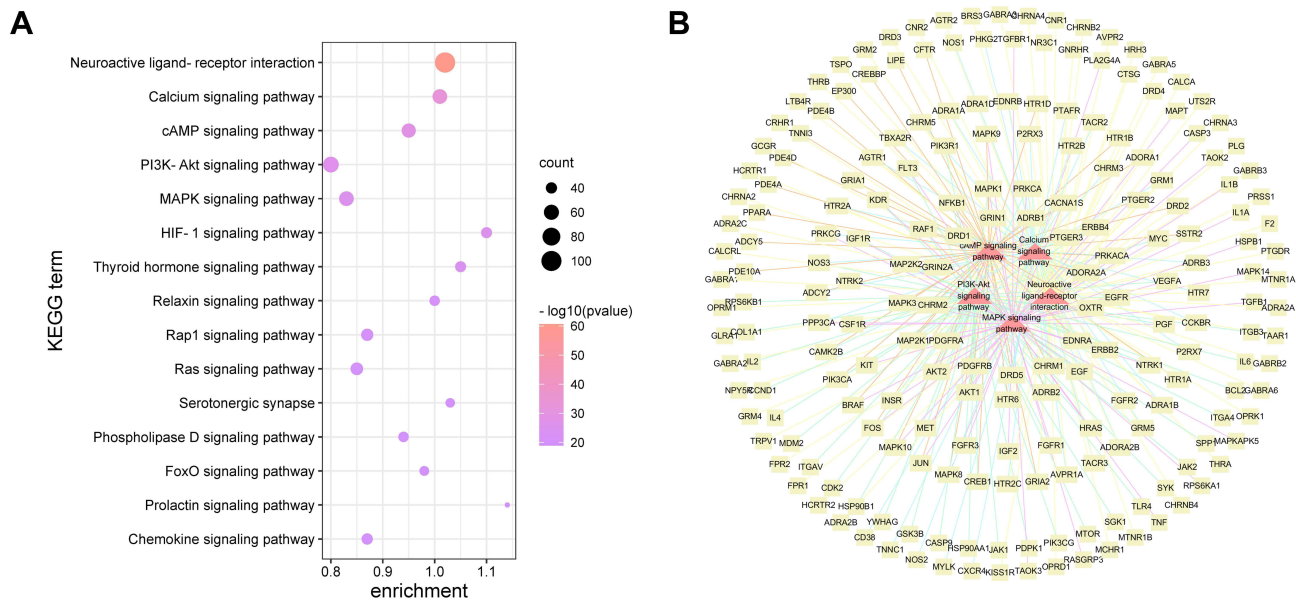


Figure 3 (A) KEGG enrichment analysis of 569 intersection targets of Wendan Decoction and Generalized Anxiety Disorder. The redder bubble is, the less P value is. **(B)** Network of top 5 KEGG pathways and their corresponding targets. Red nodes represent pathways. Yellow nodes represent related targets.

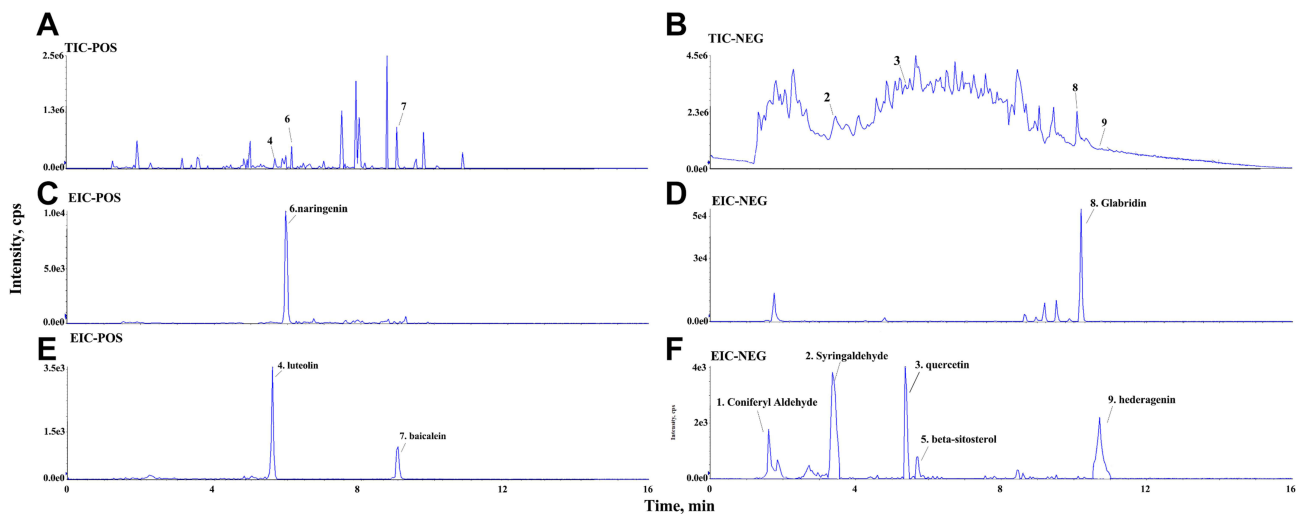


Figure 4 Identification of active ingredients of Wendan Decoction. **(A)** Total ion chromatography (TIC) on positive of Wendan Decoction. **(B)** TIC on negative of Wendan Decoction. **(C-F)** Extraction ion chromatography of Wendan Decoction. **(C)** Identification of naringenin. **(D)** Identification of glabridin. **(E)** Identification of luteolin and baicalein. **(F)** Identification of coniferyl aldehyde, syringaldehyde, quercetin, beta-sitosterol and hederagenin.

Effect of WDD on Mice Representations of Behavior Tests

Both open field test and elevated plus maze test were used to evaluate to what extent anxiety-like behaviors of mice were. The results indicated that model mice showed fewer time in the central zone compared with normal mice in the open field test and exhibited the stronger preference for closed arms than open arms in the elevated plus maze test. The above identified mice had developed successful anxiety-models. WDD and the positive control drug paroxetine can significantly reverse anxiety-like behaviors of mice (Figure 5).

Effect of WDD on Serum CORT

The levels of CORT in the serum of mice were measured by ELISA, which suggested that CORT in the serum of RRS model mice markedly increased. WDD and the positive control drug paroxetine can successfully decrease CORT in the serum (Figure 6).

Table I Chemical Identification of Wendan Decoction

No	RT/ (min)	Name	Formula	Ion	Cal./ (m/z)	Mea./ (m/z)	Error/ (ppm)	MS/MS	Herb
1	1.56	Coniferyl Aldehyde	C ₁₀ H ₁₀ O ₃	M-H	177.0557	177.0563	9.485	177.0563	Bambusa tuldoides Munro
2	3.39	Syringaldehyde	C ₉ H ₁₀ O ₄	M-H	181.0506	181.051	8.09	181.051, 121.0471	Bambusa tuldoides Munro
3	5.37	Quercetin	C ₁₅ H ₁₀ O ₇	M-H	301.0353	301.0351	2.727	301.0351, 151.0012, 107.0213	Ziziphus jujuba Mill., Glycyrrhiza uralensis Fisch. ex DC.
4	5.58	Luteolin	C ₁₅ H ₁₀ O ₆	M +H	287.055	287.0553	0.994	287.0553, 153.0176	Citrus aurantium L.
5	5.68	Beta-sitosterol	C ₂₉ H ₅₀ O	M-H	413.3788	413.3779	0.26	413.3779	Pinellia ternata (Thunb.) Makino, Zingiber officinale Roscoe, Ziziphus jujuba Mill.
6	5.96	Naringenin	C ₁₅ H ₁₂ O ₅	M +H	273.0757	273.0761	1.282	273.0761, 153.0188, 119.0496	Citrus reticulata Blanco, Citrus aurantium L., Glycyrrhiza uralensis Fisch. ex DC.
7	9.06	Baicalein	C ₂₁ H ₁₈ O ₁₁	M +H	447.0921	447.0928	1.369	447.0928, 271.0601	Pinellia ternata (Thunb.) Makino
8	10.20	Glabridin	C ₂₀ H ₂₀ O ₄	M-H	323.1288	323.1293	4.687	323.1293, 147.1480	Glycyrrhiza uralensis Fisch. ex DC.
9	10.70	Hederagenin	C ₃₀ H ₄₈ O ₄	M-H	471.3479	471.3484	3.211	471.3484, 407.3361	Poria cocos (Schw.) Wolf

Effect of WDD on Lymphocyte Subpopulations Positive for IL-6 in the Peripheral Blood

The cell markers CD3, CD4 and IL-6 were assayed using flow cytometry to differentiate between CD3⁺T lymphocyte subpopulations, CD3⁺ CD4⁺T lymphocyte subpopulations and CD4⁺ IL-6⁺T lymphocyte subpopulations in peripheral blood. After mice underwent RRS, their peripheral blood showed no significant changes in CD3⁺T lymphocyte subpopulations, CD3⁺ CD4⁺T lymphocyte subpopulations, but the proportion of CD4⁺ IL-6⁺ lymphocytes was remarkably increased. After the intervention of WDD and paroxetine, the proportion of CD4⁺ IL-6⁺ lymphocytes decreased (Figure 7). The above proved that inflammatory response was activated after RRS but partly inactivated by WDD and paroxetine.

Effect of WDD on the Vitality of BV2 Cells

Different concentrations of WDD were used to intervene in BV2 cells. It was found that the proliferation of BV2 cells was inhibited significantly when the concentration was higher than 700 µg/mL (Figure 8). Thus, 700 µg/mL was selected as the maximum concentration of WDD against BV2 cells, with 350 µg/mL to be the medium concentration and 175 µg/mL to be the low concentration, for subsequent experiments.

Effect of WDD on the Secretion of Inflammatory Factors in IL-6 Stimulated BV2 Cells

After BV2 cells were stimulated with 10 ng/mL of IL-6, the inflammatory factors TNF-α, IL-1β and PGE₂ were significantly increased in the cell supernatant, and the change was reversed by WDD with a dose-dependent effect. The positive control drug DEX at the concentration of 100 µmol/L was also able to inhibit the secretion of these inflammatory factors (Figure 9).

Effect of WDD on PI3K/AKT and MAPK Pathways in IL-6 Stimulated BV2 Cells

After the stimulation of BV2 cells with 10 ng/mL IL-6, the phosphorylation levels of PI3K, AKT and MAPK p38 were significantly increased, suggesting that the PI3K/AKT and MAPK signaling pathways were abnormally

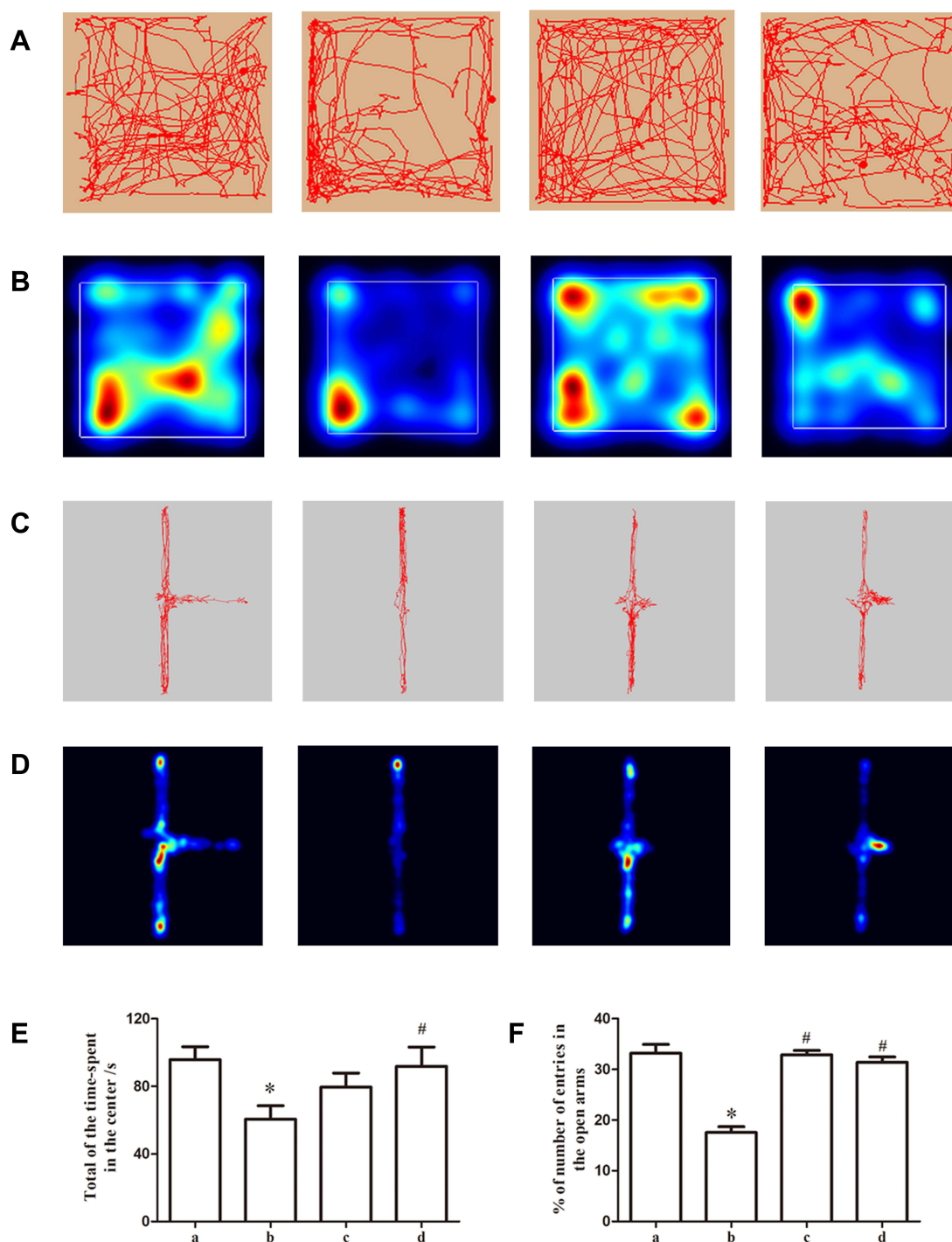


Figure 5 Behavioristic changes of mice in each group. **(A)** Representative trajectory diagram of each group in open field test. **(B)** Representative heat maps of the movement of each group in open field test. **(C)** Representative trajectory diagram of each group in elevated plus maze. **(D)** Representative heat maps of the movement of each group in elevated plus maze. **(E)** Total time spent in the central zone of open field. **(F)** Percentage of number of entries in the open arms. (a) blank control group; (b) repeated restraint stress (RRS) model group; (c) Wendan Decoction group; (d) paroxetine group. *P < 0.05, compared with blank control group; #P < 0.05, compared with RRS model group.

activated. WDD was able to reverse the phosphorylation levels of these key proteins with a dose-dependent effect. As a positive control drug, DEX at 100 $\mu\text{mol/L}$ also exerted the inhibitory effect that was superior to the high dose of WDD (Figure 10).

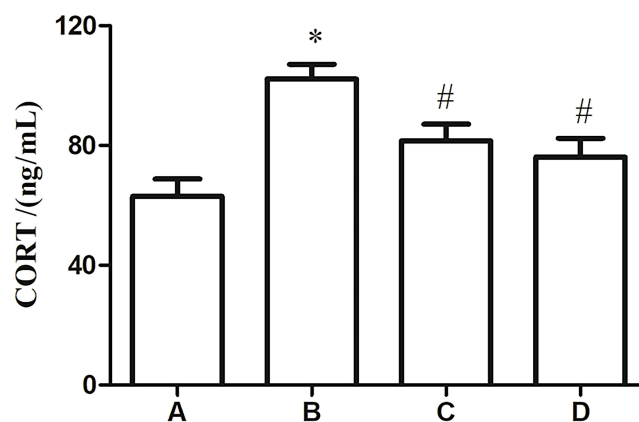


Figure 6 Plasma corticosterone concentration of mice in each group. (A) blank control group; (B) repeated restraint stress (RRS) model group; (C) Wendan Decoction group; (D) paroxetine group. *P < 0.05, compared with blank control group; #P < 0.05, compared with RRS model group.

Discussion

Persistent chronic stress abnormally activates the HPA axis, which is an important factor in the development of chronic inflammatory responses and anxiety.^{50–53} Repeated restraint stress (RRS) model is established by imposing sustained stress response on animals through long-term restraint typically used to stimulate GAD that is accompanied by hypercortisolism and anxiety-like behaviors.⁵⁴ In the present study, we established a mouse model of RRS based on previous literature and found that RRS models spent shorter dwell times in the central zones (open field test) and in the open arms (EPM test) than normal mice, as well as exhibited a significant increase in serum corticosterone. The above reflected that the model was successfully replicated and was adequate for subsequent experiments.⁵⁵ The abnormalities in ethology and corticosteroids of RRS mice were effectively reversed by WDD and the positive control drug paroxetine, suggesting that WDD is used as an antidepressant.

To further investigate therapeutic mechanism of WDD against GAD, network pharmacology was employed to predict the molecules, targets and signaling pathways that play a key role in the course of treatment. By means of network pharmacology, we determined the core ingredients with the most targets of each herb, including beta-sitosterol, baicalein, luteolin, naringenin, coniferyl aldehyde, syringaldehyde, hederagenin, quercetin, glabridin. LC-MS found that all these molecules were present in the aqueous extract of WDD we prepared. After a systematic literature search, naringenin,⁵⁶ quercetin,^{57,58} glabridin,⁵⁹ beta-sitosterol,⁶⁰ luteolin^{61,62} of them was the candidate molecule for anxiety. Among them, the anxiolytic effects of quercetin, luteolin and narigenin are closely related to the inhibition of inflammatory response, suggesting that inhibition of inflammatory response may be the potential mechanism of Wendan Decoction in treating GAD.^{57,61}

The PPI results reveal that IL-6, TNF, SRC and AKT1 are the key targets of WDD in the treatment of GAD. KEGG enrichment analysis suggests that mechanism of WDD for GAD treatment is closely correlated with neuroactive ligand receptor interaction, calcium signaling pathway, cAMP signaling pathway, PI3K/AKT signaling pathway and MAPK signaling pathway. In lymphocytes, SRC kinase regulates the transcription and synthesis of IL-6 and TNF- α by regulating downstream AKT phosphorylation and by activating the NF- κ B signaling pathway. In the central nervous system, inflammatory factors activate the PI3K/AKT and MAPK signaling pathways in microglia via the calcium and cAMP signaling pathways, and further exacerbate the inflammatory response in the central nervous system by promoting the synthesis of new inflammatory factors.^{63,64} Previous studies have shown that IL-6 is closely related to anxiety, and its activation of inflammatory responses in the central system may be a key mechanism for the occurrence and development of anxiety.^{65,66} In summary, stress contributes to inflammation of the peripheral and central nervous system mediated by IL-6, resulting in anxiety disorder. WDD might exert an anti-anxiety effect through anti-inflammation pharmacological effects (Figure 11).

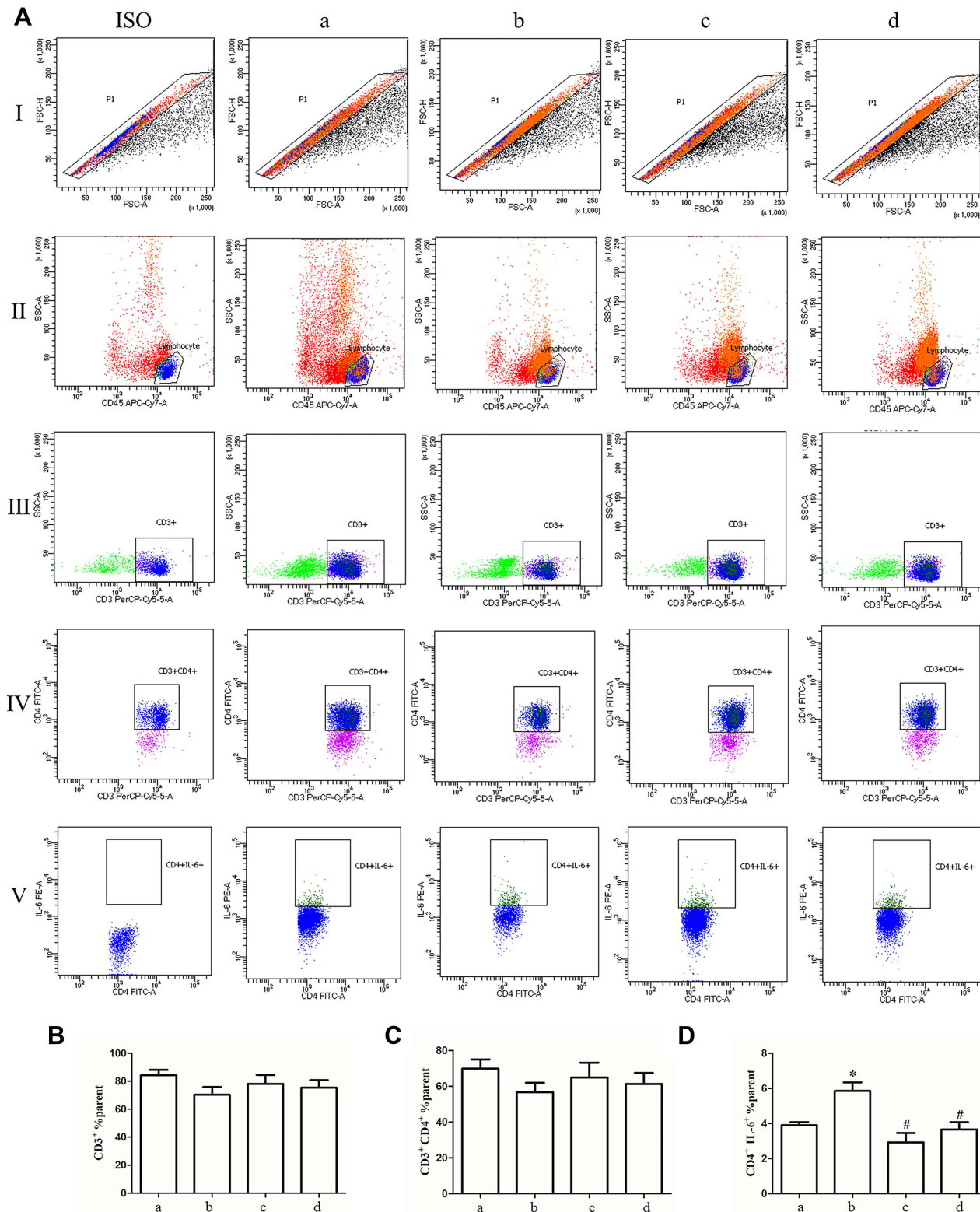


Figure 7 Percent of IL-6⁺ T lymphocytes in blood of mice in each group. (A) Representative flow cytometric analysis. (I) Sorting cell fragments and cells; (II) Sorting cells and T lymphocytes; (III) sorting T lymphocytes and CD3⁺ T lymphocytes; (IV) Sorting CD3⁺ T lymphocytes and CD3⁺ CD4⁺ T lymphocytes; (V) Sorting CD3⁺ CD4⁺ T lymphocytes and IL-6⁺ CD4⁺ T lymphocytes. (B) The proportion of CD3⁺ lymphocytes. (C) The proportion of CD4⁺ lymphocytes. (D) The proportion of IL-6⁺ CD4⁺ T lymphocytes. (a) blank control group; (b) repeated restraint stress (RRS) model group; (c) Wendan Decoction group; (d) paroxetine group. *P < 0.05, compared with blank control group; #P < 0.05, compared with RRS model group.

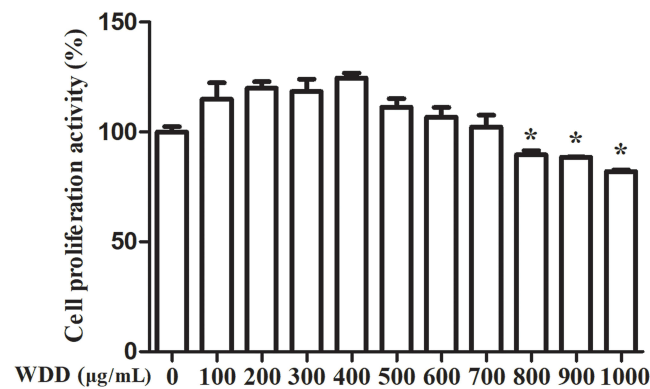


Figure 8 Effects of different concentrations of Wendan Decoction (WDD) on BV2 microglial cell proliferation. * $P < 0.05$, the proliferation of BV2 cells was inhibited, compared with blank control group.

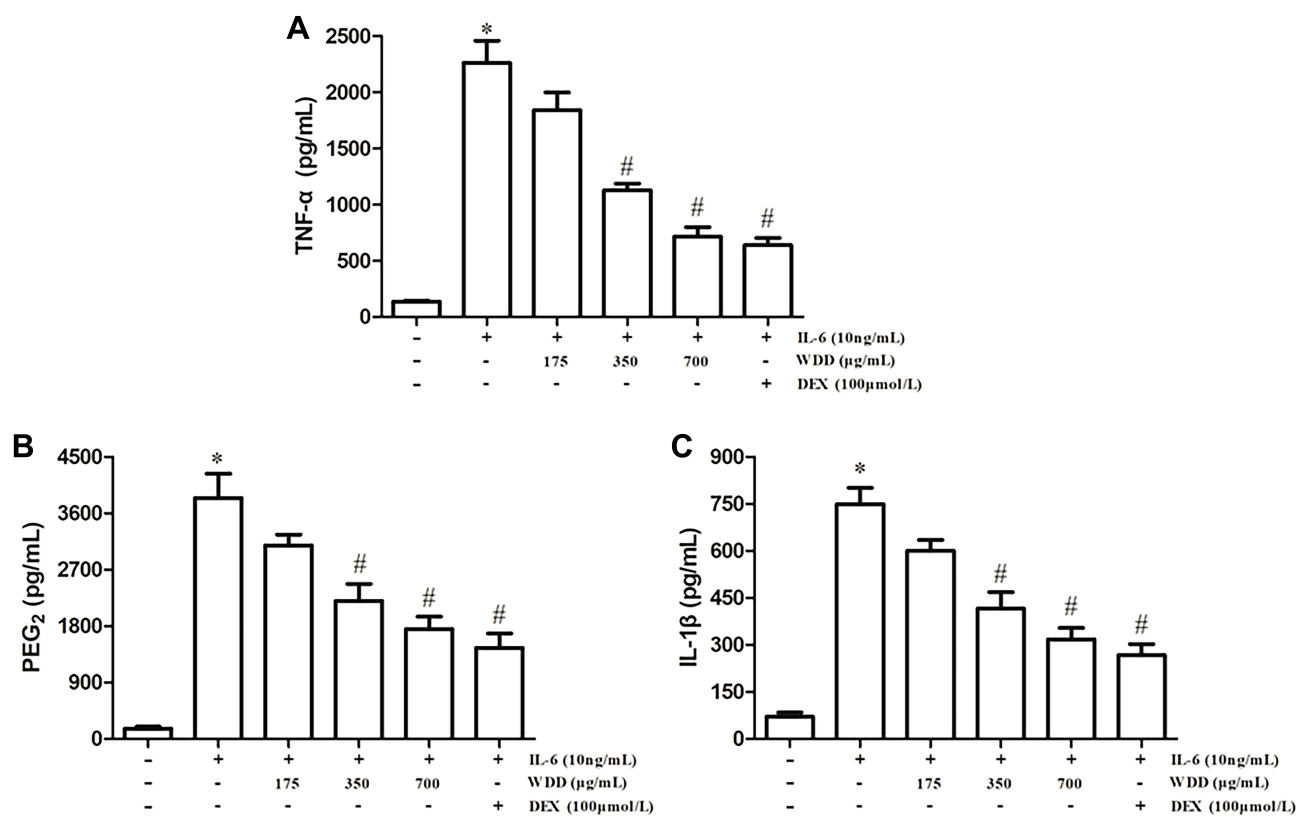


Figure 9 Effect of different concentrations of Wendan Decoction (WDD) and 100μmol/L Dexamethasone (DEX) on pro-inflammatory factors of IL-6 induced BV-2 microglia cells, respectively. (A) Concentrations of TNF-α in the cell supernatants. (B) Concentrations of PEG₂ in the cell supernatants. (C) Concentrations of IL-1β in the cell supernatants. * $P < 0.05$, compared with blank control group; # $P < 0.05$, compared with IL-6-induced group.

In the *in vivo* experiments, we measured the proportion of lymphocytes positive for IL-6 in the peripheral blood of mice by flow cytometry. The results showed that the proportion of lymphocytes positive for IL-6 was elevated in RRS mice, suggesting an activated peripheral inflammatory response in this model. WDD and Paroxetine can inhibit the above change. In the *in vitro* experiments, we stimulated BV2 cells (an immortalized mouse glial cell) by IL-6, whose results showed that IL-6 could significantly increase the ratio of p-PI3K/PI3K, p-AKT/AKT and p-p38/p38,

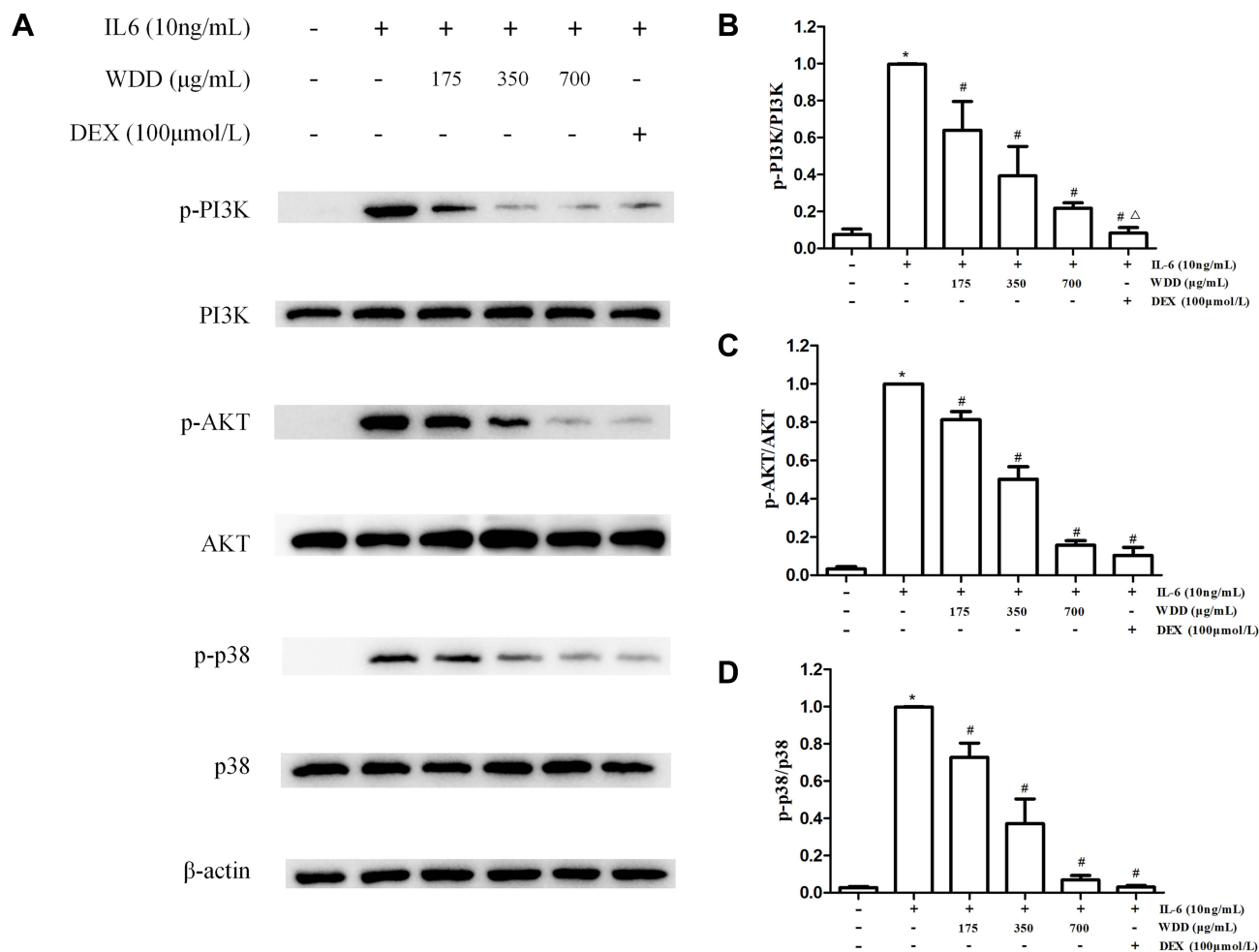


Figure 10 Effect of different concentrations of Wendan Decoction (WDD) and 100 $\mu\text{mol/L}$ Dexamethasone (DEX) on PI3K/AKT and MAPK signaling pathways of IL-6 induced BV-2 microglia cells. **(A)** Western blots of PI3K, p-PI3K, AKT, p-AKT, MAPK p38 and p-MAPK p38. **(B)** Quantification analysis of p-PI3K/PI3K. **(C)** Quantification analysis of p-AKT/AKT. **(D)** Quantification analysis of p-p38/p38. * $P < 0.05$, compared with blank control group; # $P < 0.05$, compared with IL-6-induced group; $\Delta P < 0.05$, compared with 700 $\mu\text{g/mL}$ WDD intervention group.

indicating that PI3K/AKT signaling pathway and MAPK signaling pathway were activated. Simultaneously, the inflammatory factors IL-1 β , TNF- α and PGE₂ markedly enhanced. The activation of these inflammatory pathways and the release of inflammatory factors could be reversed by WDD and positive control drugs. It is suggested that WDD may inhibit the process of aseptic inflammatory response caused by anxiety to some extent.

Limitations

However, there are limitations in our study. We only verified that WDD could inhibit the inflammation in the peripheral and central nervous system. KEGG analysis reported that neuroactive ligand-receptor interaction pathway plays an important role in the treatment of WDD against GAD. Activated microglia may overproduce the inflammatory cytokines, leading to neuronal apoptosis, neurotransmitter dysfunction and intensifying anxiety.^{67,68} In the future, we would explore the potential pharmacological mechanism of WDD against GAD through neuroactive ligand-receptor interaction.

Conclusion

In summary, animal experiments confirmed that WDD is a potent prescription to improve anxiety-like behavior and plasma corticosterone level. Subsequent network pharmacology predicts that anti-inflammation might be the mechanism of WDD for GAD treatment. In vivo, we revealed that WDD can decrease the ratio of CD4⁺IL-6⁺ T cells triggered by

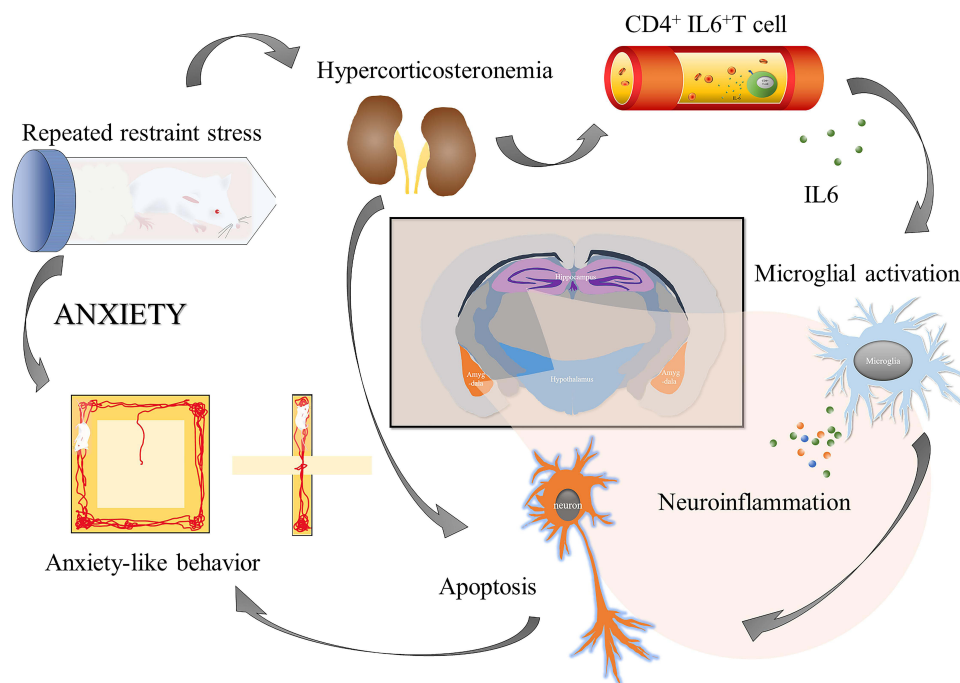


Figure 11 The hypothesis of Wendan Decoction treating Generalized Anxiety Disorder.

RRS. While in vitro, WDD can inhibit microglia activation from IL-6 stimulation. Taken together, the possible pharmacological mechanism of WDD against GAD is anti-inflammation mediated through IL-6.

Abbreviations

GAD, Generalized Anxiety Disorder; SSRIs, Serotonin Reuptake Inhibitor; SNRIs, Serotonin-norepinephrine reuptake Inhibitor; TCM, Traditional Chinese medicine; RCT, randomized controlled trials; WDD, Wendan Decoction; HAMA, Hamilton Anxiety Scale; SAS, Self-Rating Anxiety Scale; TCMSP, Traditional Chinese Medicine Systems Pharmacology database; ETCM, The Encyclopedia of Traditional Chinese Medicine database; UniProt, Unified Protein Database; OMIM, Online Mendelian Inheritance in Man database; NCA, network topology analysis; BC, Betweenness Centrality; CC, Closeness Centrality; DC, Degree Centrality; EC, Eigenvector Centrality; HRP, horseradish peroxidase; LC-MS, liquid chromatography tandem mass spectrometry; ReSpect, RIKEN MSn spectral database for phytochemicals; GNPS, Global Natural Products Social Molecular Networking; SPF, Specific Pathogen Free; RRS, repeated restraint stress; ELISA, Enzyme-linked immunosorbent assay; WB, western blot; OFT, Open field test; EPM, elevated plus maze; OD, optical density; BCA, bicinchoninic acid; DEX, Dexamethasone.

Funding

This work was supported by the National Natural Science Foundation of China (81874427) and Beijing College Student Innovation and Entrepreneurship Training Program (S202210026006).

Disclosure

All authors declare no conflict of interest.

References

1. Jeremy DM, Gayatri P, Fancher TL. Generalized anxiety disorder. *Ann Intern Med.* 2019;170(7):ITC49–ITC64. doi:10.7326/AITC201904020
2. Ruscio AM, Hallion LS, Carmen CW. Cross-sectional comparison of the epidemiology of DSM-5 generalized anxiety disorder across the globe. *JAMA Psychiatry.* 2017;74(5):465–475. doi:10.1001/jamapsychiatry.2017.0056

3. Wang X, Lin J, Liu Q, et al. Major depressive disorder comorbid with general anxiety disorder: associations among neuroticism, adult stress, and the inflammatory index. *J Psychiatr Res.* 2022;148:307–314. doi:10.1016/j.jpsychires.2022.02.013
4. GBD 2017 Disease and Injury Incidence and Prevalence Collaborators. Global, regional, and national incidence, prevalence, and years lived with disability for 354 diseases and injuries for 195 countries and territories, 1990–2017: a systematic analysis for the Global Burden of Disease Study. *The Lancet.* 2018;392(10159):1789–1858.
5. Strawn JR, Geraciotti L, Rajdev N, et al. Pharmacotherapy for generalized anxiety disorder in adult and pediatric patients: an evidence-based treatment review. *Expert Opin Pharmacother.* 2018;19(10):1057–1070. doi:10.1080/14656566.2018.1491966
6. Hengartner MP, Amendola S, Kaminski JA, et al. Suicide risk with selective serotonin reuptake inhibitors and other new-generation antidepressants in adults: a systematic review and meta-analysis of observational studies. *Epidemiol Community Health.* 2021;75(6):523–530. doi:10.1136/jech-2020-214611
7. Daitch C. Cognitive behavioral therapy, mindfulness, and hypnosis as treatment methods for generalized anxiety disorder. *Am J Clin Hypn.* 2018;61(1):57–69. doi:10.1080/00029157.2018.1458594
8. Barić H, Đorđević V, Cerovečki I, et al. Complementary and alternative medicine treatments for generalized anxiety disorder: systematic review and meta-analysis of randomized controlled trials. *Adv Ther.* 2018;35(3):261–288. doi:10.1007/s12325-018-0680-6
9. Hu J, Teng J, Wang W, et al. Clinical efficacy and safety of traditional Chinese medicine Xiao Yao San in insomnia combined with anxiety. *Medicine.* 2021;100(43):e27608. doi:10.1097/MD.00000000000027608
10. Liu P-L, Song A-R, Dong C-D, et al. Network pharmacology study on the mechanism of the herb pair of prepared Rehmannia root-Chinese arborvitae kernel for anxiety disorders. *Ann Palliat Med.* 2021;10(3):3313–3327. doi:10.21037/apm-21-531
11. Yuan Z, Hong-Xia Z, Ying XU, et al. [Network analysis and experimental verification of Qingyan Formula in treatment of perimenopausal anxiety disorder]. *Zhongguo Zhong Yao Za Zhi.* 2020;45(17):4129–4139. doi:10.19540/j.cnki.cjmm.20200622.401. Chinese.
12. Shufang Q. Observation on curative effect of Modified Chaiqin Wendan Decoction on liver depression and phlegm-fire type insomnia. *World J Sleep Med.* 2021;8(06):978–980.
13. Wu J, An H, Li Y, Duan L. TCM treatment with the modified wendan tang in 40 cases of melancholia. *J Tradit Chin Med.* 1999;19(4):296–297.
14. Huang -C-C, Chiang P-Y, Cheng Y-C, et al. Efficacy and safety of wendan decoction for acute brain injury: a randomized controlled study. *J Altern Complement Med.* 2020;26(5):392–397. doi:10.1089/acm.2019.0349
15. Che Y-W, Yao K-Y, Xi Y-P, et al. Wendan decoction for treatment of schizophrenia: a systematic review of randomized controlled trials. *Chin J Integr Med.* 2016;22(4):302–310. doi:10.1007/s11655-015-2047-z
16. Lijuan C, Zhiming Z. Clinical effect of Jiawei Wendan Decoction combined with Tandospirone in treatment of generalized anxiety disorder with bile stagnation and phlegm disturbance. *J Clin Rational Drug Use.* 2021;14(35):100–102.
17. Diao YJ, Sun SM, Liang N, et al. Clinical effect of Wendan Decoction on coronary artery disease of phlegm heat and blood stasis syndrome accompanied with anxiety and depression and influence of blood hsCRP. *Jilin J Chin Med.* 2020;40(02):193–196.
18. Zhang W, Chen Y, Jiang H, et al. Integrated strategy for accurately screening biomarkers based on metabolomics coupled with network pharmacology. *Talanta.* 2020;211(2020):120710.
19. Ru J, Li P, Wang J, et al. TCMSP: a database of systems pharmacology for drug discovery from herbal medicines. *J Cheminform.* 2014;6:13.
20. Xu HY, Zhang YQ, Liu ZM, et al. ETCM: an encyclopaedia of traditional Chinese medicine. *Nucleic Acids Res.* 2019;47(D1):D976–D982.
21. Kim S. Exploring Chemical Information in PubChem. *Curr Protoc.* 2021;1(8):e217.
22. Daina A, Michielin O, Zoete V. SwissTargetPrediction: updated data and new features for efficient prediction of protein targets of small molecules. *Nucleic Acids Res.* 2019;47(W1):W357–W364.
23. UniProt Consortium. UniProt: the universal protein knowledgebase in 2021. *Nucleic Acids Res.* 2021;49(D1):D480–D489.
24. Stelzer G, Rosen N, Plaschkes I, et al. The GeneCards Suite: from Gene Data Mining to Disease Genome Sequence Analyses. *Curr Protoc Bioinformatics.* 2016;54:1.30.1–1.30.33.
25. Amberger JS, Hamosh A. Searching Online Mendelian Inheritance in Man (OMIM): a knowledgebase of human genes and genetic phenotypes. *Curr Protoc Bioinformatics.* 2017;58:1.2.1–1.2.12.
26. Doncheva NT, Morris JH, Gorodkin J, et al. Cytoscape StringApp: network analysis and visualization of proteomics data. *J Proteome Res.* 2019;18(2):623–632.
27. Szklarczyk D, Gable AL, Nastou KC, et al. The STRING database in 2021: customizable protein-protein networks, and functional characterization of user-uploaded gene/measurement sets. *Nucleic Acids Res.* 2021;49(D1):D605–D612.
28. Yu G, Luo Z, Zhou Y, et al. Uncovering the pharmacological mechanism of *Carthamus tinctorius* L. on cardiovascular disease by a systems pharmacology approach. *Biomed Pharmacother.* 2019;117:109094.
29. Tang Y, Li M, Wang J, et al. CytoNCA: a cytoscape plugin for centrality analysis and evaluation of protein interaction networks. *Biosystems.* 2015;127:67–72.
30. Kanehisa M, Furumichi M, Tanabe M, et al. KEGG: new perspectives on genomes, pathways, diseases and drugs. *Nucleic Acids Res.* 2017;45(D1):D353–D361.
31. Lu F, Yang H, Lin SD, et al. Cyclic peptide extracts derived from *pseudostellaria heterophylla* ameliorates COPD via regulation of the TLR4/MyD88 pathway proteins. *Front Pharmacol.* 2020;11:850.
32. Morán-Santibañez K, Peña-Hernández MA, Cruz-Suárez LE, et al. Virucidal and synergistic activity of polyphenol-rich extracts of seaweeds against measles virus. *Viruses.* 2018;10(9):465.
33. Tsugawa H, Cajka T, Kind T, et al. MS-DIAL: data-independent MS/MS deconvolution for comprehensive metabolome analysis. *Nat Methods.* 2015;12(6):523–526.
34. Horai H, Arita M, Kanaya S, et al. MassBank: a public repository for sharing mass spectral data for life sciences. *J Mass Spectrom.* 2010;45(7):703–714.
35. Sawada Y, Nakabayashi R, Yamada Y, et al. RIKEN tandem mass spectral database (ReSpect) for phytochemicals: a plant-specific MS/MS-based data resource and database. *Phytochemistry.* 2012;82:38–45.
36. Wang M, Carver JJ, Phelan VV, et al. Sharing and community curation of mass spectrometry data with Global Natural Products Social Molecular Networking. *Nat Biotechnol.* 2016;34(8):828–837.

37. Wen D, Tan RZ, Zhao CY, et al. Astragalus mongholicus Bunge and Panax notoginseng (Burkill) F.H. Chen Formula for Renal Injury in Diabetic Nephropathy-In Vivo and In Vitro Evidence for Autophagy Regulation. *Front Pharmacol.* 2020;11:732.
38. Chiu CH, Chyau CC, Chen CC, et al. Erinacine A-Enriched Hericium erinaceus Mycelium produces antidepressant-like effects through modulating BDNF/PI3K/Akt/GSK-3 β signaling in mice. *Int J Mol Sci.* 2018;19(2):341.
39. Moreno-Martínez S, Tendilla-Beltrán H, Sandoval V, Flores G, Terrón JA. Chronic restraint stress induces anxiety-like behavior and remodeling of dendritic spines in the central nucleus of the amygdala. *Behav Brain Res.* 2022;7(416):113523.
40. Wang L, Yin C, Liu T, et al. Pellino1 regulates neuropathic pain as well as microglial activation through the regulation of MAPK/NF- κ B signaling in the spinal cord. *J Neuroinflammation.* 2020;17(1):83.
41. Chen GY, Chen JQ, Liu XY, et al. Total flavonoids of rhizoma drynariae restore the MMP/TIMP balance in models of osteoarthritis by inhibiting the activation of the NF- κ B and PI3K/AKT pathways. *Evid Based Complement Alternat Med.* 2021;2021:6634837.
42. Lin LY, Zhang J, Dai XM, et al. Early-life stress leads to impaired spatial learning and memory in middle-aged ApoE4-TR mice. *Mol Neurodegener.* 2016;11(1):51.
43. Wu Y, Qi F, Song D, et al. Prenatal influenza vaccination rescues impairments of social behavior and lamination in a mouse model of autism. *J Neuroinflammation.* 2018;15(1):228.
44. Oron O, Getselter D, Shohat S, et al. Gene network analysis reveals a role for striatal glutamatergic receptors in dysregulated risk-assessment behavior of autism mouse models. *Transl Psychiatry.* 2019;9(1):257.
45. Grillo CA, Piroli GG, Lawrence RC, et al. Hippocampal insulin resistance impairs spatial learning and synaptic plasticity. *Diabetes.* 2015;64(11):3927–3936.
46. Xu J, Lu C, Liu Z, et al. Schizandrin B protects LPS-induced sepsis via TLR4/NF- κ B/MyD88 signaling pathway. *Am J Transl Res.* 2018;10(4):1155–1163.
47. Chen GY, Luo J, Liu Y, et al. Network pharmacology analysis and experimental validation to investigate the mechanism of total flavonoids of rhizoma drynariae in treating rheumatoid arthritis. *Drug Des Devel Ther.* 2022;8(16):1743–1766.
48. Uriarte M, Sen Nkwe N, Tremblay R, et al. Starvation-induced proteasome assemblies in the nucleus link amino acid supply to apoptosis. *Nat Commun.* 2021;12(1):6984.
49. Guallar D, Bi X, Pardavila JA, et al. RNA-dependent chromatin targeting of TET2 for endogenous retrovirus control in pluripotent stem cells. *Nat Genet.* 2018;50(3):443–451.
50. Juruena MF, Erer F, Cleare AJ, et al. The role of early life stress in HPA axis and anxiety. *Adv Exp Med Biol.* 2020;1191:141–153.
51. Han YM, Kim MS, Jo J, et al. Decoding the temporal nature of brain GR activity in the NF κ B signal transition leading to depressive-like behavior. *Mol Psychiatry.* 2021;26(9):5087–5096.
52. Padival MA, Blume SR, Rosenkranz JA. Repeated restraint stress exerts different impact on structure of neurons in the lateral and basal nuclei of the amygdala. *Neuroscience.* 2013;246:230–242.
53. Liu WZ, Zhang WH, Zheng ZH, et al. Identification of a prefrontal cortex-to-amygdala pathway for chronic stress-induced anxiety. *Nat Commun.* 2020;11(1):2221.
54. Kumar V, Bhat ZA, Kumar D. Animal models of anxiety: a comprehensive review. *J Pharmacol Toxicol Methods.* 2013;68(2):175–183.
55. Shoji H, Miyakawa T. Differential effects of stress exposure via two types of restraint apparatuses on behavior and plasma corticosterone level in inbred male BALB/cAJcl mice. *Neuropsychopharmacol Rep.* 2020;40(1):73–84.
56. Olugbemide AS, Ben-Azu B, Bakre AG, et al. Naringenin improves depressive- and anxiety-like behaviors in mice exposed to repeated hypoxic stress through modulation of oxido-inflammatory mediators and NF- κ B/BDNF expressions. *Brain Res Bull.* 2021;169:214–227.
57. Chen F, Sun J, Chen C, et al. Quercetin mitigates methamphetamine-induced anxiety-like behavior through ameliorating mitochondrial dysfunction and neuroinflammation. *Front Mol Neurosci.* 2022;28(15):829886.
58. Zhang JL, Liu M, Cui W, et al. Quercetin affects shoaling and anxiety behaviors in zebrafish: involvement of neuroinflammation and neuron apoptosis. *Fish Shellfish Immunol.* 2020;105:359–368.
59. Hoffmann KM, Beltrán L, Ziemba PM, et al. Potentiating effect of glabridin from Glycyrrhiza glabra on GABAA receptors. *Biochem Biophys Rep.* 2016;16(6):197–202.
60. Panayotis N, Freund PA, Marvaldi L, et al. β -sitosterol reduces anxiety and synergizes with established anxiolytic drugs in mice. *Cell Rep Med.* 2021;2(5):100281.
61. Akinrinde AS, Adebisi OE. Neuroprotection by luteolin and gallic acid against cobalt chloride-induced behavioural, morphological and neurochemical alterations in Wistar rats. *Neurotoxicology.* 2019;74:252–263.
62. Crupi R, Paterniti I, Ahmad A, et al. Effects of palmitoylethanolamide and luteolin in an animal model of anxiety/depression. *CNS Neurol Disord Drug Targets.* 2013;12(7):989–1001.
63. Feng N, Jia Y, Huang X. Exosomes from adipose-derived stem cells alleviate neural injury caused by microglia activation via suppressing NF- κ B and MAPK pathway. *J Neuroimmunol.* 2019;334:576996.
64. Song FJ, Zeng KW, Chen JF, et al. Extract of Fructus Schisandrae chinensis inhibits neuroinflammation mediator production from microglia via NF- κ B and MAPK pathways. *Chin J Integr Med.* 2019;25(2):131–138.
65. Qing H, Desrouleaux R, Israni-Winger K, et al. Origin and function of stress-induced IL-6 in murine models. *Cell.* 2020;182(2):372–387.e14.
66. Gumusoglu SB, Fine RS, Murray SJ, et al. The role of IL-6 in neurodevelopment after prenatal stress. *Brain Behav Immun.* 2017;65:274–283.
67. Parul MA, Singh S, Singh S, et al. Chronic unpredictable stress negatively regulates hippocampal neurogenesis and promote anxious depression-like behavior via upregulating apoptosis and inflammatory signals in adult rats. *Brain Res Bull.* 2021;172:164–179.
68. Wang X, Wang Z, Cao J, et al. Melatonin ameliorates anxiety-like behaviors induced by sleep deprivation in mice: role of oxidative stress, neuroinflammation, autophagy and apoptosis. *Brain Res Bull.* 2021;174:161–172.

Drug Design, Development and Therapy

Dovepress

Publish your work in this journal

Drug Design, Development and Therapy is an international, peer-reviewed open-access journal that spans the spectrum of drug design and development through to clinical applications. Clinical outcomes, patient safety, and programs for the development and effective, safe, and sustained use of medicines are a feature of the journal, which has also been accepted for indexing on PubMed Central. The manuscript management system is completely online and includes a very quick and fair peer-review system, which is all easy to use. Visit <http://www.dovepress.com/testimonials.php> to read real quotes from published authors.

Submit your manuscript here: <https://www.dovepress.com/drug-design-development-and-therapy-journal>